Loss of trefoil factor 2 sensitizes rat pups to systemic infection with the neonatal pathogen *Escherichia coli* K1

Alex J. McCarthy,[1¶] George M. H. Birchenough,[2] & Peter W. Taylor[1*]

[1]School of Pharmacy, University College London, London, United Kingdom

[2]Department of Medical Biochemistry, University of Gothenburg, Gothenburg, Sweden

[*]Correspondence to Peter Taylor: peter.taylor@ucl.ac.uk

Short title: Tff2 and *E. coli* K1 neonatal infection

[¶]**Current address:** Department of Medical Microbiology, University Medical Centre Utrecht, Heidelberglaan 100, 3584 CX, Utrecht, The Netherlands

ABSTRACT

Gastrointestinal (GI) colonization of two-day-old (P2) rat pups with *Escherichia coli* K1 results in translocation of the colonizing bacteria across the small intestine, bacteremia and invasion of the meninges, with animals frequently succumbing to lethal infection. Infection but not colonization is strongly age dependent: pups become progressively less susceptible to infection over the P2-P9 period. Colonization leads to strong down-regulation of the gene encoding trefoil factor 2 (Tff2), preventing maturation of the protective mucus barrier in the small intestine. Trefoil factors promote mucosal homeostasis. We investigated the contribution of Tff2 to protection of the neonatal rat from *E. coli* K1 bacteremia and tissue invasion. Deletion of *tff2*, using CRISPR-Cas9, sensitized P9 pups to *E. coli* K1 bacteremia. There were no differences between *tff2-/-* homozygotes and wildtype with regard to the dynamics of GI colonization. Loss of capacity to elaborate Tff2 did not impact on GI tract integrity or thickness of the small intestinal mucus layer but, in contrast to P9 wildtype pups, enabled *E. coli* K1 bacteria to gain access to epithelial surfaces in the distal region of the small intestine and exploit an intracellular route across the epithelial monolayer to enter the blood circulation *via* the mesenteric lymphatic system. Although primarily associated with the mammalian gastric mucosa, we conclude that loss of Tff2 in the developing neonatal small intestine enables the opportunistic neonatal pathogen *E. coli* K1 to enter the compromised mucus layer in the distal small intestine prior to systemic invasion and infection.

INTRODUCTION

Although *Escherichia coli* are ubiquitous commensal inhabitants of the human gastrointestinal (GI) tract, some strains of this versatile species display a capacity to cause severe GI and extra-intestinal infections. Some are well adapted opportunistic pathogens that cause systemic infection in vulnerable hosts. For example, strains expressing the polysialic acid K1 capsule are harmless constituents of the adult GI tract but may cause life-threatening septicemia, sepsis and meningitis in the newborn infant following transmission from mother to neonate at or shortly after birth (1, 2). Maternally-derived *E. coli* K1 colonize the GI tract of the susceptible neonate; bacteria from the GI-colonizing cohort may translocate from the gut lumen to the blood, eliciting symptoms of sepsis and septic shock (2), and then invade the central nervous system to induce inflammation of the meninges (3).

The strong age dependency associated with *E. coli* K1 human systemic infection can be replicated in the neonatal rat (4, 5). Oral administration of K1 bacteria to two-day-old (P2) pups initiates stable colonization of the GI tract and lethal systemic infection develops due to the capacity of a small number of *E. coli* K1 bacteria to translocate across the epithelium of the middle section of the small intestine (MSI) to the submucosa, avoid capture by the mesenteric lymphatic system, enter the blood circulation and establish infection in the brain and other organs (6-9). Pups become progressively less susceptible to systemic infection when colonized over the P2-P9 period, even though GI colonization can be established as readily in resistant P9 animals as in susceptible P2 pups (5). In P2 animals, the mucus barrier of the small intestine is poorly developed, allowing *E. coli* K1 bacteria to gain access to the enterocyte surface of the MSI lumen and translocate through the epithelial cell monolayer by an intracellular pathway to the submucosa (8). The protective mucus layer matures to full thickness over P2-P9, coincident with the development of resistance to infection. At P9, K1 bacteria are physically separated from villi by the mucus layer and their numbers controlled by mucus-embedded antimicrobial peptides, preventing invasion of host tissues.

P2 and P9 pups respond differently to the threat posed by colonizing *E. coli* K1, reflecting substantial changes in developmental gene expression *postpartum* (10). A large number of genes expressed in the GI tract were up- (241 for P2, 354 for P9) or down-regulated (36 for P2, 240 for P9) following initiation of colonization but the transcriptomic responses were very different, with virtually no commonality of modulation of gene expression between the two age groups. Notably, α-defensin genes *defa24* and *defa-rs1* were up-regulated in P9 GI tissues in response to colonization, but no changes in α-defensin gene expression occurred in the P2 GI tract. These mucus-embedded antimicrobial peptides are produced by Paneth cells and contribute to the barrier function of the mucus layer (11), as evidenced by the demonstration that chemical ablation of Paneth cells reduces the GI concentration of α-defensins and sensitizes normally resistant P9 pups to systemic infection (8).

Conversely, developmental expression of the gene encoding trefoil factor 2 (Tff2) was highly down-regulated by *E. coli* K1 colonization in P2 but not in P9 rats; no evidence for modulation of *tff1* and *tff3*, genes for other members of the trefoil factor family, was found (10). Mucin-associated trefoil factor proteins mediate maintenance and restoration of GI mucosal homeostasis, stabilising the mucus layer, enhancing intestinal epithelial repair and responding to GI mucosal injury and inflammation (12, 13). As *tff2* expression in the GI tract (including stomach) of non-colonized neonates increases incrementally over P1-P9, with a substantial decline from P9 to P11 (10), it is likely that *tff2* down-regulation induced by *E. coli* K1 colonization will further compromise innate GI defenses in susceptible P2 pups. In adult humans (14) and rodents (15), Tff2 appears to be associated primarily with the stomach and duodenum, although intravenously administered Tff2 also distributes rapidly to Paneth cells in the small intestine and to crypt colonic cells before appearing within the associated mucus layer (16). Tff1 is localized predominantly in gastric foveolar cells and surface epithelium throughout the stomach (17) and Tff3 within goblet cells of the small intestine and colon (18), although species differences are evident (19) and these structurally related proteins may be functionally interchangeable (13). Little is known of the roles or distribution of

trefoil factors during GI maturation. Trefoil mRNAs are expressed in early embryonic rat intestine and stomach before overt differentiation of epithelial cells (20); Tff3 appears around gestational day 17 in the rat intestine and increases further postnatally and during the weaning period (21). These observations provide further evidence that the mucosal barrier is not fully formed at birth and may render the neonate vulnerable to infection following colonisation of the GI tract.

In this study we examine the role of the *tff2* gene product in protection of the neonatal rat from experimental systemic infection using a *tff2-/-* knockout rat. We show that P9 pups, normally resistant to infection due to the barrier function of the MSI mucus, become vulnerable to bacteremia following GI colonization with *E. coli* K1 strain A192PP and we relate this to changes in GI tract physiology elicited by lack of Tff2.

RESULTS

Tff2 rat knockout. *tff2* knockout Sprague-Dawley rats were generated commercially using the Clustered Regularly Interspaced Short Palindromic Repeats (CRISPR)-Cas9 system (22). Non-proprietary details are described in Experimental Procedures. gRNA1 was targeted to exon 1 and gRNA11 was targeted to exon 3 (Fig. S1A). Four rats bearing *tff2* mutations were identified and confirmed by PCR-mediated amplification and sequencing analysis (Fig. S1B). We backcrossed founder 2 that carried the most extensive deletion (1933 bp) with a wildtype (WT) Sprague-Dawley rat (Fig. S1C). The resulting F1 heterozygotes were identified by PCR-mediated genotyping and were subsequently crossed. F2 *tff2*-/- homozygotes were identified, and homozygote breeding colonies were maintained. Previous studies have demonstrated higher *tff2* expression in stomach compared to intestinal tissues in humans and rats (14, 23). Expression of *rps23* and *tff2* genes was therefore measured using qRT-PCR analysis of stomach samples from wildtype and *tff2-/-* animals. There was a 16-fold reduction in stomach *tff2* gene expression in *tff2-/-* homozygotes compared to WT rats (Fig. S1D), indicative of a knock-down in *tff2* gene expression. We were unable to detect sufficient Tff2 protein in tissue extracts by Western blot and therefore could not directly compare Tff2 content

of WT and *tff2-/-* tissues. Homozygote litters comprised 3-20 neonatal pups and all animals appeared healthy, gained weight in identical fashion to WT pups of comparable age and were maintained in healthy condition for up to three months. As loss of Tff2 could compromise defences against bacterial invasion of the rodent GI tract (10, 12, 24), we examined changes in expression of genes encoding selected proteins known to impact on GI tract protection. Thus, genes encoding Tff1 and Tff3 (*tff1*, *tff3*), the α-defensins DefaRS1 and Defa24 (*defaRS1*, *defa24*) and tumour necrosis factor‑alpha (*tfna*) were up-regulated 0.5-3.5-fold in the proximal (PSI), MSI and distal (DSI) regions of the P9 small intestine compared to their expression in WT P9 rat pups (Fig. 1). In contrast to *tff1*, *tff3* and *tfna*, the two α-defensin genes were down-regulated in colonic tissue; these antimicrobial peptides are known to play a role in the small intestine rather than the colon (25). Conversely, the interferon-gamma gene (*ifng*) was marginally down-regulated in the small intestine and marginally up-regulated in the colon. Thus, there appears to be some re-programming of antimicrobial defences in the neonatal GI tract following knockout of *tff2*, against a background of developmental modulation of trefoil factor expression in the stomach, PSI, MSI, DSI and colon during the immediate *postpartum* period (Figs. 1 & S2).

Susceptibility of *tff2-/-* rat pups to *E. coli* K1 infection. Colonization of each member of a litter of P2 Sprague-Dawley rat pups by oral administration of 2–6 × 10^6 CFU *E. coli* K1 strain A192PP resulted in disseminated systemic infection in highly comparable fashion to our previous data obtained using Wistar rats (5, 26). Pups become progressively less susceptible to infection after colonization over the P2-P9 period and by P8-P9 are resistant even though the degree of GI colonization is comparable to P2 susceptible neonates (8, 26). As expected, WT Sprague-Dawley rats that received a single colonizing dose at P9 did not succumb to infection. In contrast, *tff2-/-* pups colonized at P9 exhibited significantly increased susceptibility to the neonatal pathogen (Fig. 2A). Although a proportion of colonized *tff2-/-* pups survived for the 25 day observation period without significant symptoms, all pups examined were bacteremic by day 7 after oral administration of the colonizing dose (Fig. 2B); only a small proportion of WT pups displayed bacteremia during the first two days following

initiation of colonization. To confirm that systemic invasive disease arose in *tff2*-/- but not WT neonates, we tracked colonization and invasion in P9 pups using the well-characterised bioluminescent isogenic strain *E. coli* A192PP-*lux* (27) and 2D bioluminescent imaging (Figs. 2C &2D). The bioluminescent signals from the torso foci were comparable between WT and *tff2-/-,* suggesting that the total bacterial load in the intestine and/or colon is comparable. We then measured bioluminescent signals eight days after colonization, a time point at which we anticipated that *tff2-/-* pups would be bacteremic and WT pups abacteremic. Wider systemic bioluminescent signals were only detected in *tff2-/-* pups; notably, the bioluminescent signal from the head region was significantly higher in *tff2-/-* compared to WT pups (Figs. 2C & 2D), most probably reflecting meningeal colonization and/or invasion (7). This data confirms that *tff2*-/- P9 pups were more susceptible to systemic invasive infection than wildtype P9 pups. The extent of GI colonization of the PSI, MSI and DSI as well as colon and the mesenteric lymphatic system of *tff2-/-* P9 pups was comparable to WT, with only a small but significant difference in CFU in the DSI 24 h after initiation of colonization (Fig. 3).

GI integrity and the mucus layer in *tff2-/-* neonatal rats. As colonizing bacteria disseminate from the *tff2-/-* neonatal gut, the barrier function of the GI tract of non-colonized P9 animals was determined by oral administration of small molecule (FITC, 389 Da) and polymeric (FITC-dextran, 4 kDa) fluorescent probes and quantification of serum fluorescence for 4 h after feeding of the probes (Fig. 4A). There were no significant differences in the uptake of either probe; increased susceptibility to systemic infection of *tff2-/-* neonates is therefore unlikely to be due to a non-specific increase in intestinal permeability. The small increases in uptake of both probes over the 4 h incubation period are most likely due to macropinocytosis of luminal content by neonatal enterocytes (8, 28, 29). Similarly, histological analysis demonstrated that there were no differences in the synthesis or secretion of the major mucus structural protein Muc2, as determined by immunostaining using antibodies detecting intracellular Apo-Muc2 (Fig. 4B) or the mature secreted protein (Fig. 4C). Thus, we could detect no differences in the appearance of either the small intestinal or colonic mucus

layer between WT and *tff2-/-* neonates that would reflect changes in intestinal integrity. In similar fashion, H&E staining failed to reveal any abnormalities in the appearance of tissues from regions of the GI tract (Fig. S3).

Enterocyte-internalised *E. coli* A192PP are found only in the distal portion of the small intestine. *E. coli* K1 bacteria cross the epithelial barrier and gain access to the blood circulation with low frequency (6, 8, 9). We searched for bacteria expressing the O18 LPS antigen in Methacarn-fixed sections of the small intestine and colon of WT and *tff2-/-* pups 48 h after colonization with *E. coli* A192PP (O18:K1) at P9. We employed a commercial O18 antibody; bacteria in GI tissues from non-colonized wildtype and *tff2-/-* P9 animals failed to react with this antibody, indicating that no bacteria expressing the O18 antigen were present in detectable numbers in these tissue samples. No O18 antigen was found in close association with epithelial cells in the small intestine of WT P9 rat pups and the dense population of O18 antigen-bearing *E. coli* A192PP in the colon was kept at a distance from the enterocytes lining the lumen (Fig. 5A) by the thick mucus layer in this region of the GI tract (Fig. 4C). In contrast, O18 bacteria were consistently found in close proximity to the GI epithelium in the DSI but not PSI, MSI or colon of *tff2-/-* pups and O18 staining showed bacteria at locations deep within the mucus layer (Figs. 5A & 5B). Higher magnification images indicated that some of these bacteria were contained within intracellular compartments and were present in numbers suggestive of replication within vesicles (Fig. 5B). Analysis of DSI tissue sections clearly demonstrated a significantly higher number of tissue associated O18-positive bacterial cells in *tff2-/-* compared to WT neonates (Fig. 5C). We have previously shown that ablation of Paneth cells sensitizes resistant pups to *E. coli* A192PP small intestinal infection (8). We therefore assessed the possibility that Paneth cell function was compromised in the *tff2-/-* DSI by quantifying Apo-Muc2 positive cells present at the epithelial crypt base (Figs. 5D & 5E); however, no differences between WT and *tff2-/-* tissues were detected. Together, this data indicates that colonizing *E. coli* K1 bacteria gain entry to the systemic circulation in *tff2-/-* rats by exploiting a transcellular route across the DSI that contrasts with the MSI-restricted transepithelial route adopted by *E. coli* A192PP in susceptible

WT P2 neonatal rat pups (8). Intriguingly, the capacity of the pathogen to infect the DSI of neonates lacking Tff2 appears to be independent of the postnatal mucus barrier formation that is thought to confer resistance in WT neonates.

DISCUSSION

Initiation of GI colonization of P2 rat pups with *E. coli* A192PP elicited a substantial (26.4-fold) downregulation of *tff2* in the GI tract within twelve hours of bacterial seeding; there was no modulation of expression of other genes encoding trefoil factors or of those involved in GI mucus homeostasis (10). The susceptibility of P9 *tff2-/-* knockouts to bacteremia and, in the majority of cases, lethality (Fig 2) supported our earlier microarray data (10) indicating that Tff2 contributes to mucosal barrier function in the small intestine by ensuring that potentially invasive bacteria are unable to make close contact with the epithelial surface. *E. coli* K1 bacteria were found in close proximity to epithelial surfaces within the DSI region of the P9 *tff2-/-* GI tract and appeared to gain entry to the blood circulation by an intracellular route (Fig. 5). At least some bacteria accessing the submucosal space were able to avoid capture by the mesenteric lymphatic system to cause systemic infection. Mucosal barrier function appeared to be lost only in the DSI, in contrast to WT P2 pups in which GI transit occurred in the MSI (8). The lesion enabling *E. coli* A192PP to interact with the DSI epithelial surface was clearly discrete: we detected no histological changes in this region attributable to loss of *tff2* and no increase in overall GI permeability. Although the invading bacteria were able to penetrate the DSI mucus layer, in contrast to the P9 wildtype, there were no differences in mucosal thickness, morphological appearance or Paneth cell numbers, as determined by immunohistochemistry, that could account for increased susceptibility to invasive infection. In addition, there were no major differences in the numbers of colonizing bacteria and their distribution in the GI tract between P9 wildtype and *tff2-/-* animals (Fig. 3), indicating that Tff2 played no significant role in controlling the population of colonizing *E. coli* K1 bacteria. It has been reported that basal gastric acid secretion is increased and gastric mucosal thickness decreased in

otherwise healthy *tff2-/-* mice (30). For technical reasons, *tff2- /-* homozygotes were generated in Sprague-Dawley rats. Our previous studies of susceptibility of the neonatal rat to *E. coli* K1 infection have been undertaken in Wistar rats and although we compared the dynamics of infection following *E. coli* A192PP colonization in both breeds and found no qualitative or quantitative differences in susceptibility, this should be borne in mind when comparing our previous work with data from this study.

Tff2, as the naturally occurring dimer, is most frequently found in association with the mammalian gastric mucosa (13, 31) but has been reported in human adult pancreatic, colonic and skeletal tissues (14). PCR has indicated that *tff2* gene expression is less restricted, with relatively low expression in human (14) and rat (15) small intestinal tissue and the partial redistribution of intravenously administered Tff2 to the mucus layer of the small intestine (16) suggests a capacity to interact in *situ* with Muc2, the predominant intestinal mucin. Our data (Fig. S2) confirm *tff2* expression in all regions of the small intestine and suggest that loss of capacity to elaborate Tff2 in the P9 rat DSI leads to loss of mucosal barrier function even though the mucus layer appears normal. In the stomach, Tff2 is secreted in concert with Muc6 by deep gastric glands and the gastric glycoform binds with high specificity to O-linked α1,4-GlcNAc-capped hexasaccharides on Muc6-rich stomach mucus (24). These motifs could facilitate Tff2 binding in other regions of the GI tract, particularly during embryonic and early *postpartum* development. We attempted to localize Tff1, Tff2 and Tff3 in regions of the GI tract from wildtype and *tff2-/-* homozygotes whilst preserving the integrity of the mucus layer by Methacarn fixation, but were unable to do so as methanol-induced precipitation of these proteins abrogated their capacity to react with polyclonal antibodies (unpublished observations).

Loss of capacity to elaborate Tff2 led to upregulation in the P9 small intestine of genes associated with mucosal defense (Fig. 1) but these increases in gene expression did not prevent rapid translocation of colonizing *E. coli* K1 from the DSI to the blood compartment. Interestingly, 60% of P9 pups were bacteremic within 24 h of initiation of colonization (Fig. 2B), a significantly

faster rate compared to *E. coli* A192PP-colonized WT P2 pups (5, 8). All P2 pups succumb to lethal infection within seven days of initiation of colonization but a significant proportion of *tff2-/-* P9 pups survived for at least 25 days, in all probability reflecting maturation of other components of the GI tract defense repertoire in the older, albeit genetically compromised animals (8, 10). It is clear the GI defense in these rapidly maturing animals is a highly cooperative phenomenon and that disruption of one or more key defense determinants provides opportunities for pathogens such as *E. coli* K1 for invasion of deeper tissues (Fig. 2C) as also shown by the increased susceptibility of P8-P9 pups to infection induced by chemical ablation of Paneth cells (8).

Tff2 has been used in rodent models to repair gastric injury (32, 33) and inflammation-induced colonic damage (34). The protein is highly resistant to adverse conditions in the GI tract and in these studies was administered intravenously, intrarectally or orally, in all cases accelerating GI repair. These observations raise the possibility that exogenous administration of recombinant Tff2 could repair the lesions induced by tff2 knockout and eventually accelerate small GI tract maturation in neonates deemed at risk from opportunistic infections arising from bacterial colonization of the gut. Such an approach could be particularly relevant if suppression of *tff2* expression is a common feature of colonization of the gut of the newborn by neonatal pathogens such as *E. coli* K1.

MATERIALS AND METHODS

Bacteria. *E. coli* A192PP (O18:K1; ST95) was obtained by two rounds of serial passage through P2 rat pups of the septicemia isolate *E. coli* A192 (5, 35). The passaged derivative was significantly more virulent in the neonatal rat model of infection compared to the parent isolate (36). The strain was cultured in Luria-Bertani (LB) or Muller-Hinton (MH) broth or agar at 37^{o}C. Engineering of *E. coli* A192PP to stably and constitutively express the *Photorhabdus luminescens*-derived *lux* operon (*luxCDABE*) with minimal loss of virulence is described elsewhere (26, 36). *E. coli* A192PP-*lux* was cultured in LB media containing 50 μg/ml of kanamycin and used to colonize rat pups as described in section 4.4.

Generation of *tff2* knockout rats. *tff2* knockout Sprague-Dawley rats were generated by Horizon Discovery (St. Louis, MO, U.S.A.). In brief, two pairs of single-guide (sg) RNAs were designed to cleave together in order to generate a ~1.8kb deletion (4894 bp) between the target sites, removing the gene encoding Tff2 from the NC 005119 region of the genome. The most active sgRNAs were selected in cultured eukaryotic cells; the design and synthesis of donor DNA containing the desired mutation were facilitated by Horizon in-house bioinformatic programs and were validated by sequencing. Donor DNA along with Cas9/sgRNA reagent was delivered by microinjection into fertilized embryos to create the desired mutation; a maximum of two microinjection sessions was performed. The most potent sgRNA with minimal off-target potential was assembled into a ribonucleoprotein complex with Cas9 endonuclease and, together with the donor DNA, was delivered into zygotes from Sprague-Dawley rats followed by embryo transfer into pseudo-pregnant females. For gestation and identification of the founder mutant phase, tissue biopsies were obtained at approximately two weeks *postpartum*. Viable progeny was analyzed for the presence of the desired mutation by genomic PCR and DNA sequencing. Fifteen animals were screened and four founders contained a 1.8kb deletion; two rats were bred to the F1 heterozygous stage with wildtype Sprague-Dawley rats and nineteen F1 heterozygotes were identified as carrying the *tff2* mutation by PCR-mediated genotyping and DNA sequence analysis. Loss of Tff2 did not impact on the wellbeing of *tff2-/-* animals, at least during the first fourteen weeks of life: pups remained healthy and homozygous adults bred in comparable fashion to wildtype.

PCR. Genotyping of offspring from *tff2* mutant mating pairs was determined by PCR. For upstream sgRNA non-homologous end-joining (NHEJ) detection by sequence analysis the following primers were used: Tff2 Cel1 F1: 5’-ggagccatgtcagcatttct, Tff2 Cel1 R1: 5’-gtcctttgcgggaacataga (expected wildtype band 349bp); for downstream sgRNA NHEJ detection by sequence analysis: Tff2 Cel1 F2: 5’-ccctaagaaggcagaactgg, Tff2 Cel1 R2: 5’-acagaggcacacacagatgc (expected wildtype band 364bp); for large deletions between sgRNAs by electrophoresis analysis: Tff2 Cel1 F1: 5’-ggagccatgtcagcatttct, Tff2 Cel1 R2: 5’-acagaggcacacacagatgc (expected mutation band 341bp). Reaction mixtures (total

volume 25 µl) contained 1 µl DNA template (extracted using Epicentre QuickExtract solution), 2.5 µl of 10 µM forward primer, 2.5 µl of 10 µM reverse primer, 12.5 µl Sigma JumpStart Taq ReadyMix (P2893) and 6.5 µl H_2O. Thermal cycling was undertaken at 95°C for 5 min, followed by 35 cycles at 95°C for 30 s, 60°C for 30 s and 68°C for 40 s, with a final extension step of 5 min at 68°C. PCR products were detected following separation by electrophoresis on 2% agarose gels by staining with ethidium bromide.

Semi-quantitative reverse transcriptase (RT)-PCR was used to evaluate expression of key host genes during early (P2-P9) *postpartum* development of the neonatal rat. RNA was extracted using RNeasy Midi kit (QIAgen) and cDNA amplified from 25 ng RNA by RT-PCR: RNA was mixed with Brilliant II RT-PCR master mix (Agilent), gene-specific forward and reverse primer pairs (Table S1) and AffinityScript RT-RNase block enzyme mixture (Agilent) to a final volume of 25 µl. The thermocycling programme comprised 30 min at 50°C and 10 min at 95°C followed by 35 cycles of 30s at 95°C, 1 min at 60°C, and 30 s at 72°C. Experiments were performed using Mx3000P v2.0 software (Stratagene) to normalize SYBR1 to ROX fluorescence and to determine cycle threshold values using adaptive baseline and amplification-based threshold algorithm enhancements. Expression was examined by normalizing qRT-PCR data from non-colonized animals to RNA data obtained from non-colonized P2 intestinal tissues. qRT-PCR was undertaken as described previously (10).

Colonization of neonatal rats. Animal experiments were approved by the Ethical Committee of University College London and were conducted in accordance with national legislation under United Kingdom Home Office Project License PPL 70/7773. All experiments were conducted in accordance with the United Kingdom Animals (Scientific Procedures) Act, 1986 and the Codes of Practice for the Housing and Care of Animals used in Scientific Procedures, 1989. All animal experiments were undertaken with *E. coli* K1 A192PP or the bioluminescent derivative A192PP-*lux* (27, 37). Sprague-Dawley rats were used to generate *tff2* knockouts and served as WT controls. Susceptibility of genetically unaltered Sprague Dawley pups to infection following GI colonization was comparable to that obtained with Wistar rats in our previous studies of neonatal rat infection (8). Litters comprised

12–14 pups and were retained in a single cage with their natural mothers. The animal model of colonization and infection has been described in detail (26). Each pup was fed 20 µl of Mueller-Hinton (MH) broth culture of *E. coli* A192PP (2–6 × 10^6 CFU, 37°C) from an Eppendorf micropipette. Controls were fed 20 µl of sterile broth. Colonization was determined by MacConkey agar culture of perianal swabs and bacteremia by culture of daily blood samples taken from the footpad. Disease progression was monitored by regular evaluation of symptoms of systemic infection and pups were culled and recorded as dead once a threshold, described earlier (26), had been reached.

Intestinal permeability. GI tract permeability of rat pups was assessed using FITC and FITC-dextran (Sigma). Pups were fed 15 µl of probe solution (800 mg/ml in sterile PBS) and culled 1, 2 or 4 h after administration. Plasma fluorescence was determined against plasma from control rat pups and values normalized for total blood volume for each pup.

2D bioluminescent imaging. Quantitative bioluminescent imaging was performed using an IVIS Lumina series III (PerkinElmer) incorporating a pre-warmed imaging platform. Anaesthesia was induced with 5% isoflurane and maintained with 2.5% isoflurane. Animals were not subjected to repeated anaesthesia. Bioluminescence was measured within standardized regions of interest and data expressed as flux (photons per second), adjusted using the following formula to ensure all measurements had positive value: $\log_{10}(\text{flux} + 1)$.

Histology, immunohistochemistry and microscopy. Neonatal rats were killed by decapitation and GI tissues segmented into stomach, mesentery, colon and small intestine; 2 cm segments from proximal, middle and distal small intestine were excised without washing as described (26). Tissue samples were placed in methanol-Carnoy's fixative (Methacarn) and maintained at room temperature for at least 3 h. Paraffin-embedded sections were dewaxed and hydrated. Some sections were stained with H&E. Muc2 was stained using polyclonal rabbit antiserum raised against either non-glycosylated Apo-Muc2 protein (PH497) or mature glycosylated Muc2 protein (Muc2C3); Alexa Fluor 555/488-conjugated goat anti-rabbit IgG (ThermoFisher) was used as secondary antibody. Immunofluorescent sections were counterstained with Hoechst 33258 (Sigma). *E. coli*

A192PP was visualised in tissue sections with rabbit polyclonal antibody raised against the O18 LPS surface antigen (7). Stained sections were mounted in Prolong Anti-fade (Life Technologies); images were acquired using an LSM 700 confocal microscope equipped with an oil immersion lens and 488 nm and 555 nm lasers (Zeiss). Contact of *E. coli* A192PP with tissue was quantified by counting the number of extracellular and intracellular O18-postive cells in contact with the epithelial cell layer in x20 magnification micrograph fields.

ACKNOWLEDGMENTS

This study was funded by Medical Research Council research grant MR/K018396/1 and by Action Medical Research grant GN2075. The funders had no role in study design, data collection and interpretation, or the decision to submit the work for publication. The National Institute for Health Research University College London Hospitals Biomedical Research Centre provided infrastructural support.

381 **REFERENCES**

382 1. Sarff LD, McCracken GH, Schiffer MS, Glode MP, Robbins JB, Ørskov I, Ørskov F. 1975.
383 Epidemiology of *Escherichia coli* K1 in healthy and diseased newborns. Lancet 1(7916):1099-
384 1104.
385 2. Simonsen KA, Anderson-Berry AL, Delair SF, Davies HD. 2014. Early-onset neonatal sepsis.
386 Clin Microbiol Rev 27:21–47. https://doi.10.1128/CMR.00031-13.
387 3. Tunkel AR, Scheld WM. 1993. Pathogenesis and pathophysiology of bacterial meningitis. Clin
388 Microbiol Rev 6:118–136.
389 4. Glode MP, Sutton A, Moxon ER, Robbins JB. 1977. Pathogenesis of neonatal *Escherichia coli*
390 meningitis: induction of bacteremia and meningitis in infant rats fed *E. coli* K1. Infect Immun
391 16:75–80.
392 5. Mushtaq N, Redpath MB, Luzio JP, Taylor PW. 2004. Prevention and cure of systemic
393 *Escherichia coli* K1 infection by modification of the bacterial phenotype. Antimicrob Agents
394 Chemother 48:1503–1508.
395 6. Pluschke G, Mercer A, Kusećek B, Pohl A, Achtman M. 1983. Induction of bacteremia in
396 newborn rats by *Escherichia coli* K1 is correlated with only certain O(lipopolysaccharide)
397 antigen types. Infect Immun 39:599–608.
398 7. Zelmer A, Bowen M, Jokilammi A, Finne J, Luzio JP, Taylor PW. 2008. Differential expression
399 of the polysialyl capsule during blood-to-brain transit of neuropathogenic *Escherichia coli* K1.
400 Microbiology 154:2522-2532. https://doi.org/10.1099/mic.0.2008/017988-0.
401 8. Birchenough GMH, Dalgakiran F, Witcomb LA, Johansson MEV, McCarthy AJ, Hansson GC,
402 Taylor PW. 2017. Postnatal development of the small intestinal mucosa drives age-
403 dependent, regio-selective susceptibility to *Escherichia coli* K1 infection. Sci Rep 7:83.
404 https://doi.org/10.1038/s41598-017-00123-w.
405 9. McCarthy AJ, Stabler RA, Taylor PW. 2018. Genome-wide identification of *Escherichia coli* K1
406 genes essential for growth in vitro, gastrointestinal colonizing capacity and survival in serum

by transposon insertion sequencing. J Bacteriol 200:e00698-17. https://doi.org/10.1128/JB.00698-17.

10. Birchenough GMH, Johannson MEV, Stabler RA, Dalgakiran F, Hansson GC, Wren BW, Luzio JP, Taylor PW. 2013. Altered innate defenses in the neonatal gastrointestinal tract in response to colonization by neuropathogenic *Escherichia coli*. Infect Immun 81:3264-3275. https://doi.org/10.1128/IAI.00268-13.
11. Lehrer RI, Lu W. 2012. α-defensins in human innate immunity. Immunol Rev 245:84-112. https://doi.org/10.1111/j.1600-065X.2011.01082.x.
12. Kjellev S. 2009. The trefoil factor family—small peptides with multiple functionalities. Cell Molec Life Sci, 66:1350–1369. DOI: 10.1007/s00018-008-8646-5.
13. Aihara E, Engevik KA, Montrose MH. 2017. Trefoil factor peptides and gastrointestinal function. Ann Rev Physiol 79:357-380. https://doi.org/10.1146/annurev-physiol-021115-105447.
14. Madsen J, Nielsen O, Tornøe I, Thim L, Holmskov U. 2007. Tissue localization of human trefoil factors 1, 2, and 3. J Histochem Cytochem 55:505-513.
15. Taupin DR, Pang KC, Green SP, Giraud AS. 1995. The trefoil peptides spasmolytic polypeptide and intestinal trefoil factor are major secretory products of the rat gut. Peptides 16:1001-1005.
16. Poulsen SS, Thulesen J, Nexø E, Thim L. 1998. Distribution and metabolism of intravenously administered trefoil factor 2/porcine spasmolytic polypeptide in the rat. Gut 43:240-247.
17. Hanby AM, Poulsom R, Singh S, Elia G, Jeffery RE, Wright NA. 1993. Spasmolytic polypeptide is a major antral peptide: distribution of the trefoil peptides human spasmolytic polypeptide and pS2 in the stomach. Gastroenterology 105:1110-1116.
18. Suemori, S, Lynch-Devaney K, Podolsky DK. 1991. Identification and characterization of rat intestinal trefoil factor: tissue- and cell-specific member of the trefoil protein family. Proc Nat Acad Sci USA 88(24), 11017-11021.

19. Jiang Z, Lossie AC, Applegate TJ. 2011. Evolution of trefoil factor(s): genetic and spatio-temporal expression of trefoil factor 2 in the chicken (*Gallus gallus domesticus).* PLoS One 6:e22691. https://doi.org/10.1371/journal.pone.0022691.
20. Familari M, Cook GA, Taupin DR, Marryatt G, Yeomans ND, Giraud AS. 1998. Trefoil peptides are early markers of gastrointestinal maturation in the rat. Int J Dev Biol 42:783-789.
21. Lin J, Holzman IR, Jiang P, Babyatsky MW. 1999. Expression of intestinal trefoil factor in developing rat intestine. Biol Neonate, 76:92-97.
22. Cong L, Zhang F. 2015. Genome engineering using CRISPR-Cas9 system. Methods Molec Biol 1239:197-217. https://doi.org/10.1007/978-1-4939-1862-1_10.
23. Jeffrey GP, Oates PS, Wang TC, Babyatsky MW, Brand SJ. 1994. Spasmolytic polypeptide: a trefoil peptide secreted by rat gastric mucous cells. Gastroenterology 106:336-345.
24. Hanisch FG, Bonar D, Schloerer N, Schroten H. 2014. Human trefoil factor 2 is a lectin that binds α-GlcNAc-capped mucin glycans with antibiotic activity against *Helicobacter pylori*. J Biol Chem 289:27363-27375. https://doi.org/10.1074/jbc.M114.597757.
25. Cunliffe RN. 2003. α-defensins in the gastrointestinal tract. Molec Immunol 40:463-467.
26. Dalgakiran F, Witcomb LA, McCarthy AJ, Birchenough GMH, Taylor PW. 2014. Non-invasive model of neuropathogenic *Escherichia coli* infection in the neonatal rat. J Vis Exp 92:e52018. https://doi.org/10.3791/52018.
27. Witcomb LA, Czupryna J, Francis KP, Frankel G, Taylor PW. 2017. Non-invasive three-dimensional imaging of *Escherichia coli* K1 infection using Diffuse Light Imaging Tomography combined with Micro-Computed Tomography. Methods 127:62-68. https://doi.org/10.1016/j.ymeth.2017.05.005.
28. Forbes GB, Reina JC. 1972. Effect of age on gastrointestinal absorption (Fe, Sr, Pb) in the rat. J Nutr 102:647-652.
29. Henning SJ. 1979. Biochemistry of intestinal development. Environ Health Perspect 33:9-16.

30. Farrell JJ, Taupin D, Koh TJ, Chen D, Zhao CM, Podolsky DK, Wang TC. 2002. TFF2/SP-deficient mice show decreased gastric proliferation, increased acid secretion, and increased susceptibility to NSAID injury. J Clin Invest 109:193-204.
31. Hoffmann W. 2015. TFF2, a MUC6-binding lectin stabilizing the gastric mucus barrier and more (Review). Int J Oncol 47:806-816. https://doi.org/10.3892/ijo.2015.3090.
32. Sun Y, Wu W, Zhang Y, Lv S, Wang L, Wang S, Peng X. 2009. Stability analysis of recombinant human TFF2 and its therapeutic effect on burn-induced gastric injury in mice. Burns 35:869-874. https://doi.org/10.1016/j.burns.2008.12.002.
33. Xue L, Aihara E, Podolsky DK, Wang TC, Montrose MH. 2010. *In vivo* action of trefoil factor 2 (TFF2) to speed gastric repair is independent of cyclooxygenase. Gut 59:1184-1191. https://doi.org/10.1136/gut.2009.205625.
34. Tran CP, Cook GA, Yeomans ND, Thim L, Giraud AS. 1999. Trefoil peptide TFF2 (spasmolytic polypeptide) potently accelerates healing and reduces inflammation in a rat model of colitis. Gut 44:636-642.
35. Achtman M, Mercer A, Kusećek B, Pohl A, Heuzenroeder M, Aaronson W, Sutton A, Silver, RP. 1983. Six widespread bacterial clones among Escherichia coli K1 isolates. Infect Immun 39:315-335.
36. McCarthy AJ, Negus D, Martin P, Pechincha C, Oswald E, Stabler RA, Taylor PW. 2016. Pathoadaptive mutations of *Escherichia coli* K1 in experimental neonatal systemic infection. PLoS One 11:e0166793. https://doi.org/10.1371/journal.pone.0166793.
37. Witcomb LA, Collins JW, McCarthy AJ, Frankel G, Taylor PW. 2015. Bioluminescent imaging reveals novel patterns of colonization and invasion in systemic *Escherichia coli* K1 experimental infection in the neonatal rat. Infect Immun 83:4528-4540. https://doi.org/10.1128/IAI.00953-15.

LEGENDS

FIG. 1 *tff2* knockout rat pups increase expression of intestinal defence proteins. qRT-PCR data for *tff1*, *tff3*, *defaRS1*, *defa24*, *tnfa* and *ifng* was normalized to *rps23* gene, and data from P9 *tff2-/-* pups standardized to expression levels in P9 wildtype animals using the ΔC_T method for relative quantification of qPCR Data. Mean ± SEM; *n* = 3-5. Δ_{CT} determined by Student's *t*. ns, non-significant, **P*<0.05, ***P*<0.01. Each spot represents data from individual litter mates.

FIG. 2 Tff2-deficient neonatal rat pups exhibit increased susceptibility to *E. coli* K1 systemic infection. (A) Survival of wildtype and *tff2-/-* rats dosed orally with 2-6 x 10^6 CFU *E. coli* A192PP at P9; *n* = 13 (wildtype) and 25 (*tff2-/-*). (B) Presence of *E. coli* K1 bacteria in blood samples from pups dosed with *E. coli* A192PP at P9, determined by culture. *E. coli* K1 colonies were identified using bacteriophage K1E. Day 1, WT *n* = 12, Day 2, WT *n* = 10, Day 1 *tff2-/- n*= 11, Day 2 *tff2-/- n* = 13, Day 7 WT *n* = 12, Day 7 *tff2-/- n*= 15; χ^2 test: * p < 0.05, ** < 0.01. (C & D) 2D-bioluminescent imaging of pups dosed orally with 2-6 x 10^6 *E. coli* A192PP-*lux2* at P9. Images (C) show photoemissions collected from the entire body of live animals at day 8 after initiation of colonization (P17). (D) Distribution of bioluminescent bacteria between torso and head. Bioluminescence values were determined as $\log_{10}$ (flux+1); flux measured in photons/s. Mean ± SD (Student's *t*). *P*<0.05 (Mann Whitney U test).

FIG. 3 A comparable degree of GI colonization in wildtype (WT) and *tff2-/-* rats administered 2-6 x 10^6 CFU *E. coli* A192PP at P9. CFU in proximal (PSI), middle (MSI), distal small intestine (DSI), mesenteric lymphatics (MLN) and colon are shown (A) 24 h and (B) 48 h after initiation of colonization. All non-significant except **P*<0.05 (Mann Whitney U test). Segments of small intestine were obtained as follows (25): The small intestine was aligned from the mid-point. The last 2 cm of tissue prior to the caecum was collected as DSI, the tissue from 5 - 7 cm above the mid-point collected as the PSI, and the tissue from 3 - 5 cm below the mid-point collected as the MSI.

FIG. 4 Loss of Tff2 does not affect GI permeability or the appearance of the GI mucus layer. (A) Intestinal permeability in non-colonized P9 wildtype and *tff2-/-* pups; plasma fluorescence was

509 determined for 4 h following oral administration of FITC or FITC-Dextran. Plasma fluorescence was
510 expressed as $\log_{10}$ relative fluorescence units (RFU). (B & C) Representative confocal micrographs of
511 Methacarn-fixed proximal (PSI), middle (MSI), distal small intestinal (DSI) and colonic tissue sections
512 from non-colonised P9 wildtype (WT) and *tff2-/-* rats obtained 48 h after colonization with *E. coli*
513 A192PP at P9 and probed for Apo-Muc2 (B) and Muc2 (C). In C, red arrows in the small intestinal
514 images show secreted Muc2 and the red dashed line in the colonic images shows the approximate
515 border of the inner mucus layer. Scale bars: 100µm.

516 **FIG. 5** *E. coli* K1 bacteria gain entry to enterocytes only from the DSI. (A) Representative confocal
517 micrographs of Methacarn-fixed PSI, MSI, DSI and colonic tissue sections from wildtype (WT) and
518 *tff2-/-* neonatal rats administered 2-6 x 10^6 CFU *E. coli* A192PP at P9. Tissues were harvested 48 h
519 after initiation of colonization and sections stained for O18 LPS and DNA. No O18-positive bacteria
520 were visualised in proximity to the enterocyte layer in the DSI (B) or other regions of the WT GI tract.
521 Small numbers of O18-positive bacteria were associated with enterocytes in the *tff2-/-* DSI but not
522 with other GI tissues (A) and could be seen in intracellular locations within villi (B). (C) Quantification
523 of O18-positive bacterial cells in contact with DSI tissue of WT and *tff2-/-* neonates 24 and 48 h after
524 K1 dose. (D & E) quantification of immature Paneth cells in DSI. Sections were stained for Apo-Muc2
525 and DNA; crypt base (green dashed line) indicated. . *n* = 3-4 animals/group, mean ± SEM; **P*<0.05 as
526 determined by 2-way ANOVA and Sidak's multiple comparison.

527

528

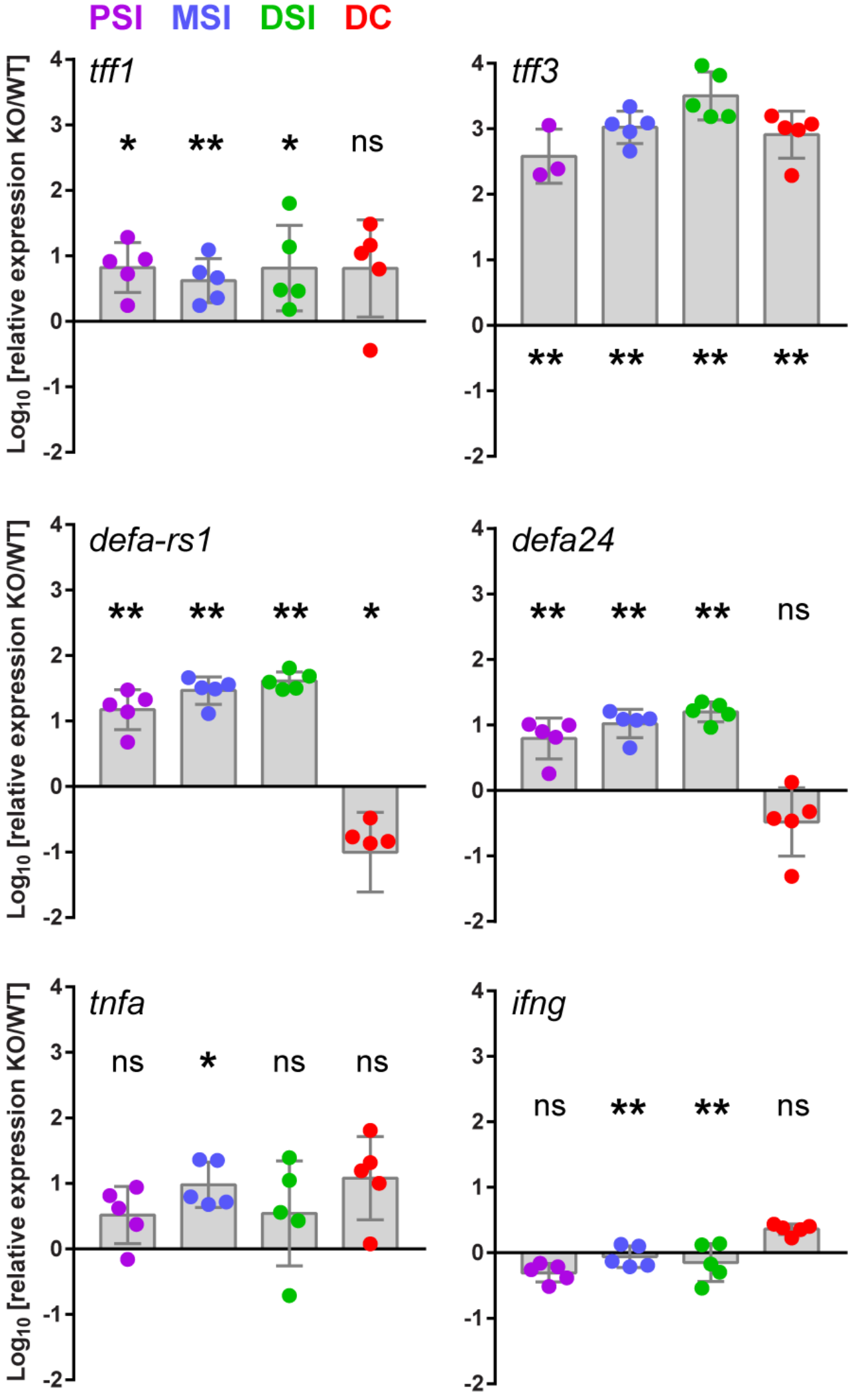
PSI
MSI
DSI
DC
tff1
tff3
defa-rs1
defa24
tnfa
ifng
Log10 [relative expression KO/WT]
4
3
2
1
0
-1
-2
*
**
*
ns
**
**
**
**
**
**
**
*
**
**
**
ns
ns
*
ns
ns
ns
**
**
ns

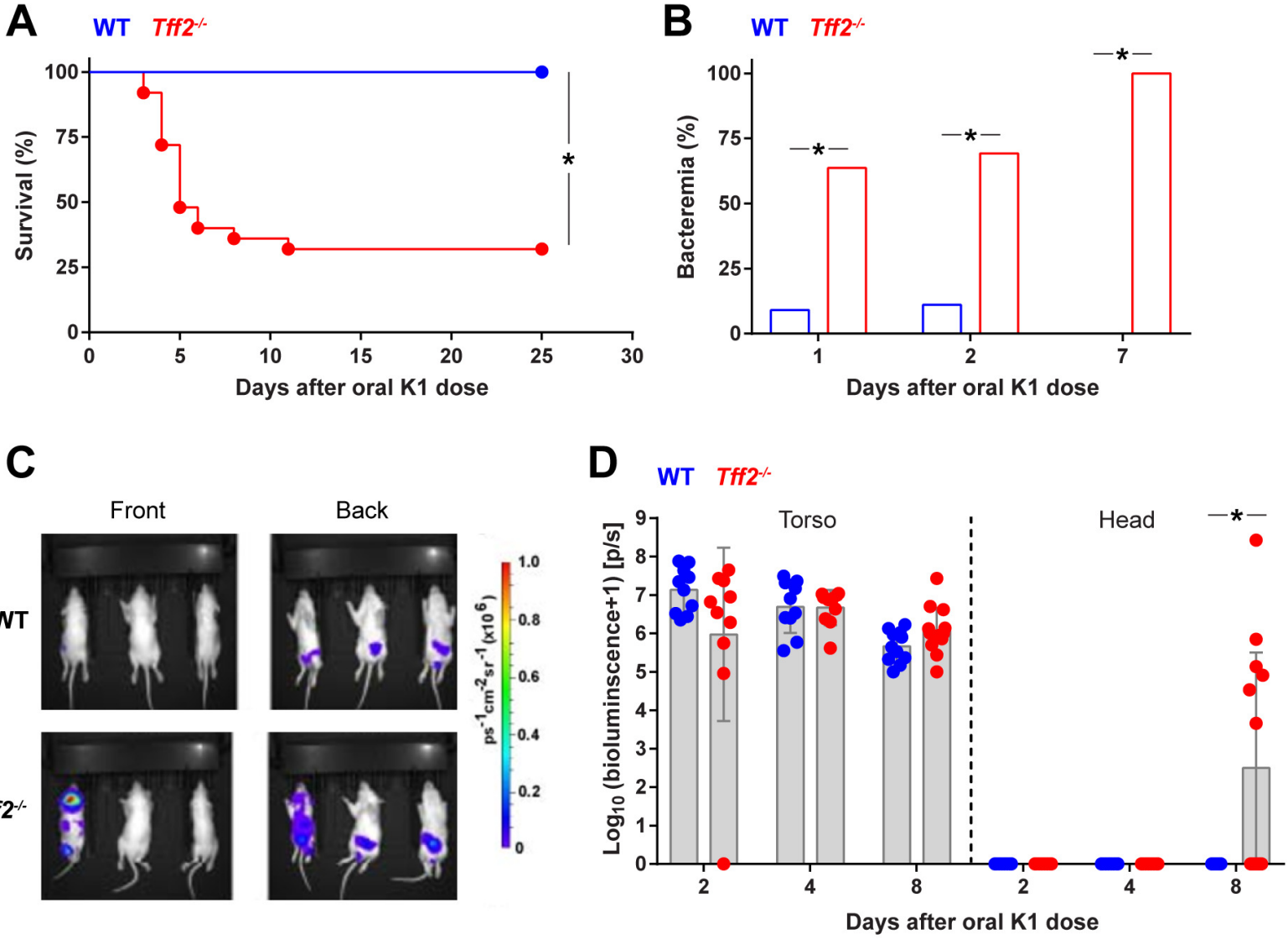
A
WT
Tff2-/-
Survival (%)
Days after oral K1 dose
*
B
WT
Tff2-/-
Bacteremia (%)
Days after oral K1 dose
C
Front
Back
WT
Tff2-/-
ps-1cm-2sr-1 (x10 6)
D
WT
Tff2-/-
Torso
Head
Log10 (bioluminscence+1) [p/s]
Days after oral K1 dose

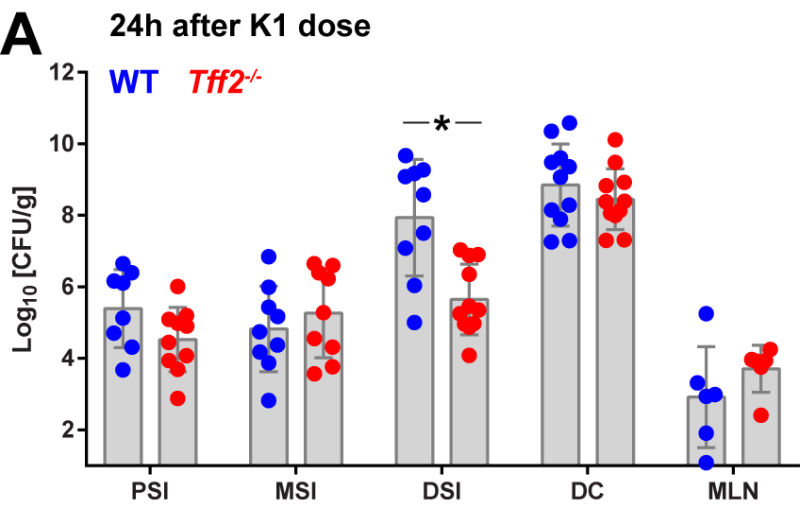
A
24h after K1 dose
WT
Tff2-/-
Log10 [CFU/g]
12
10
8
6
4
2
*
PSI
MSI
DSI
DC
MLN

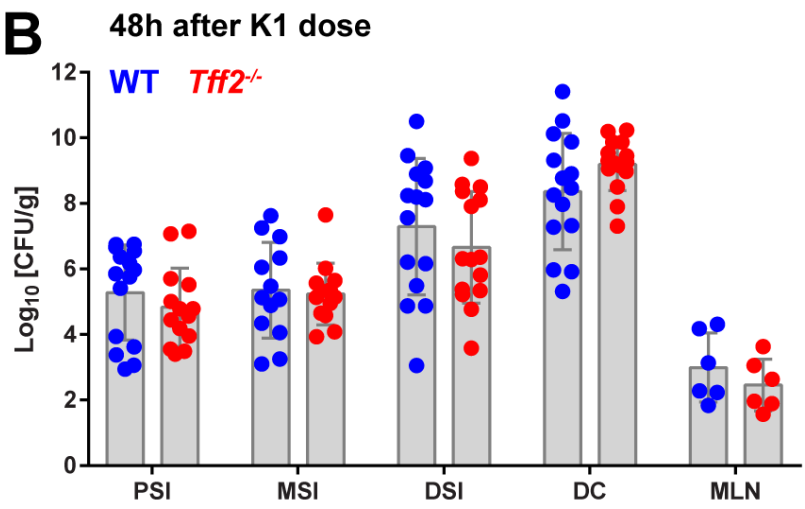
B
48h after K1 dose
WT
Tff2-/-
Log10 [CFU/g]
12
10
8
6
4
2
0
PSI
MSI
DSI
DC
MLN

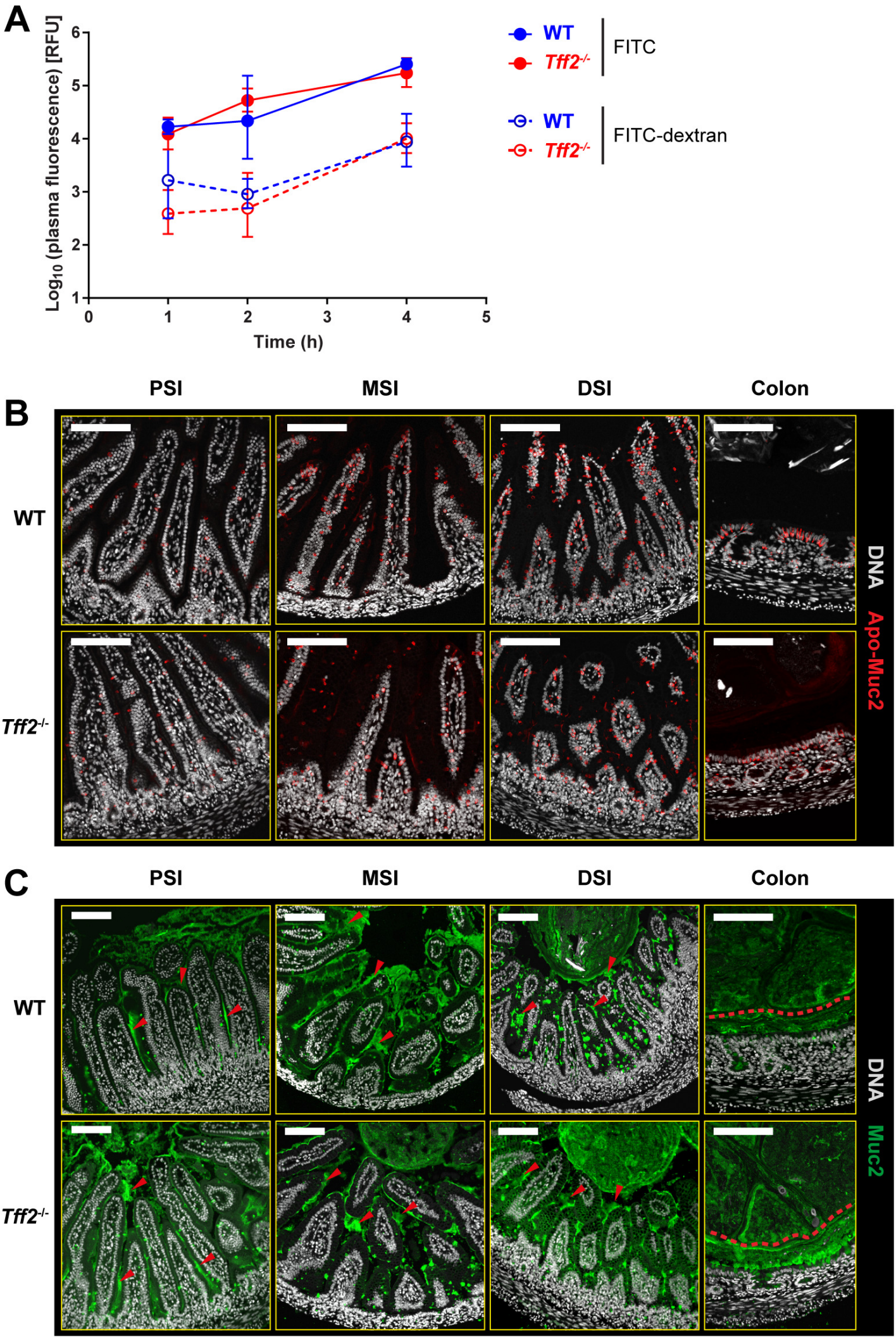
A
Log10 (plasma fluorescence) [RFU]
Time (h)
WT
Tff2-/-
FITC
WT
Tff2-/-
FITC-dextran
B
PSI
MSI
DSI
Colon
WT
Tff2-/-
DNA
Apo-Muc2
C
PSI
MSI
DSI
Colon
WT
Tff2-/-
DNA
Muc2

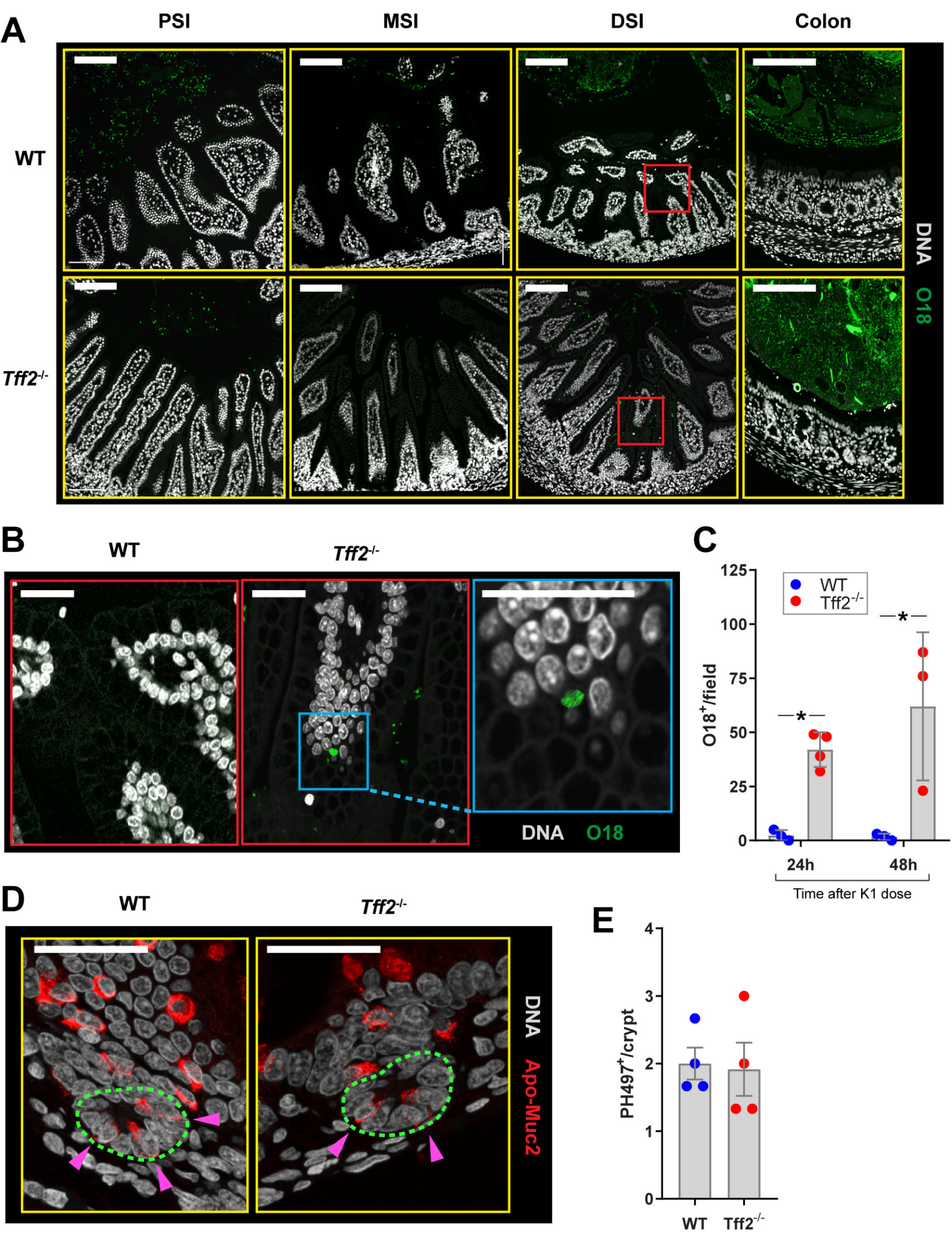
A
PSI
MSI
DSI
Colon
WT
Tff2-/-
DNA
O18
B
WT
Tff2-/-
DNA
O18
C
WT
Tff2-/-
O18+/field
125
100
75
50
25
0
*
*
24h
48h
Time after K1 dose
D
WT
Tff2-/-
DNA
Apo-Muc2
E
PH497+/crypt
4
3
2
1
0
WT
Tff2-/-